

Photonic production of P -wave states of B_c mesons

A.V. Berezhnoy, V.V. Kiselev, A.K. Likhoded
Institute for High Energy Physics, Protvino 142284, Russia
E-mail: LIKHODED@MX.IHEP.SU

Numerical calculations for the production of P -wave levels of B_c quarkonium in $\gamma\gamma$ collisions are performed in the leading $O(\alpha_s^2\alpha_{em}^2)$ order of perturbation theory. The total cross-section of P -wave state production is about 10 % of that for the S -wave levels. The contribution of fragmentation component (6 + 6 diagrams) is low, and the basic contribution is determined by the recombination mechanism (8 Feynman diagrams). The gauge invariant term of the $\bar{b} \rightarrow B_c$ fragmentation (6 diagrams) quite accurately reproduces the result of the fragmentation model, whereas there is a strong deviation of the $c \rightarrow B_c$ fragmentation term from the predictions of the fragmentation model.

I. INTRODUCTION

At present, the production mechanism for the heavy quarkonium of mixed flavour, B_c meson [1], is quite reliably predicted theoretically. The production of two pairs of heavy quarks $b\bar{b}c\bar{c}$ is calculated in the framework of perturbative QCD, whereas the hadronization of the color-singlet $\bar{b}c$ pair into the meson is described in a nonrelativistic potential model.

In e^+e^- annihilation, the analysis of leading order approximation in the perturbation theory of QCD at $M^2/s \ll 1$ allows one to derive analytical expressions for differential cross-sections of the B_c meson production being treated as the process of the $\bar{b} \rightarrow B_c$ fragmentation [2-5]. In the framework of the fragmentation mechanism, the S -wave level production dominates, and the P -wave state yield is only about 10 % with respect to the total number of produced mesons of the $(\bar{b}c)$ family. However, as it was found in photon-photon and gluon-gluon collisions [6,7], there is an additional contribution of the recombination for the S -wave states. Such a term changes spectra as well as the relative yields of pseudoscalar and vector states. The recombination mechanism can result in an enhancement of the P -wave level yield.

In this paper we consider the exact calculation of complete set of the leading order diagrams in perturbation theory for the production of the $(\bar{b}c)$ system P -wave states in $\gamma\gamma$ collisions and make a comparison of the results with the fragmentation model approximation.

II. CALCULATION TECHNIQUE

The A^{SJj_z} amplitude of the B_c meson production can be expressed through the amplitude of four free quarks production $T^{Ss_z}(p_i, k(\mathbf{q}))$ and the orbital wave function of the B_c meson, $\Psi^{Ll_z}(\mathbf{q})$, in the meson rest frame as

$$A^{SJj_z} = \int T^{Ss_z}(p_i, k(\mathbf{q})) \cdot (\Psi^{Ll_z}(\mathbf{q}))^* \cdot C_{s_z l_z}^{Jj_z} \frac{d^3\mathbf{q}}{(2\pi)^3}, \quad (1)$$

where J and j_z are the total spin of the meson and its projection on z axis in the B_c rest frame, correspondingly; L and l_z are the orbital momentum and its projection; S and s_z are the sum of quark spins and its projection; $C_{s_z l_z}^{Jj_z}$ are the Clebsh-Gordon coefficients; p_i are four-momenta of B_c , b and \bar{c} , \mathbf{q} is the three-momentum of \bar{b} quark in the B_c meson rest frame; $k(\mathbf{q})$ is the four-momentum, obtained from the four-momentum $(0, \mathbf{q})$ by the Lorentz transformation from the B_c rest frame to the system, where the calculation of $T^{Ss_z}(p_i, k(\mathbf{q}))$ is performed. Then, the four-momenta of \bar{b} and c quarks, composing the B_c meson, will be determined by the following formulae with the accuracy up to $|\mathbf{q}|^2$ terms

$$\begin{aligned} p_{\bar{b}} &= \frac{m_b}{M} P_{B_c} + k(\mathbf{q}), \\ p_c &= \frac{m_c}{M} P_{B_c} - k(\mathbf{q}), \end{aligned} \quad (2)$$

where m_b and m_c are the quark masses, $M = m_b + m_c$, and P_{B_c} is the B_c momentum. Let us note that for the P -wave states it is enough to take into account only terms, linear over \mathbf{q} in eq.(1).

The product of spinors $v_{\bar{b}}\bar{u}_c$, corresponding to the \bar{b} and c quarks in the $T^{Ss_z}(p_i, k(\mathbf{q}))$ amplitude of eq.(1), should be substituted by the projection operator

$$\mathcal{P}(\Gamma) = \sqrt{M} \left(\frac{\frac{m_b}{M} \hat{P}_{B_c} + \hat{k} - m_b}{2m_b} \right) \Gamma \left(\frac{\frac{m_c}{M} \hat{P}_{B_c} - \hat{k} + m_c}{2m_c} \right), \quad (3)$$

where $\Gamma = \gamma^5$ for $S = 0$, or $\Gamma = \hat{\varepsilon}^*(P_{B_c}, s_z)$ for $S = 1$, where $\varepsilon(P_{B_c}, s_z)$ is the polarization vector for the spin-triplet state.

For the sake of convenience, one can express the $\mathcal{P}(\Gamma)$ operator through the spinors of the following form

$$\begin{aligned} v'_b(p_b + k, \pm) &= \left(1 - \frac{\hat{k}}{2m_b} \right) v_b(p_b, \pm), \\ u'_c(p_c - k, \pm) &= \left(1 - \frac{\hat{k}}{2m_c} \right) u_c(p_c, \pm), \end{aligned} \quad (4)$$

where $v_b(p_b, \pm)$ and $u_c(p_c, \pm)$ are the spinors with the given projection of quark spin on z axis in the B_c meson rest frame. Note, that the spinors in eq.(4) satisfy the Dirac equation for the antiquark with the momentum $p_b + k$ and mass m_b or for the quark with the momentum $p_c - k$ and mass m_c up to the linear order over k (i.e. over \mathbf{q} , too), correspondingly.

One can easily show that the following equalities take place

$$\begin{aligned} \sqrt{\frac{2M}{2m_b 2m_c}} \frac{1}{\sqrt{2}} \{v'_b(p_b + k, +)\bar{u}'_c(p_c - k, +) - v'_b(p_b + k, -)\bar{u}'_c(p_c - k, -)\} &= \\ &= \mathcal{P}(\gamma^5) + O(k^2), \\ \sqrt{\frac{2M}{2m_b 2m_c}} v'_b(p_b + k, +)\bar{u}'_c(p_c - k, -) &= \\ &= \mathcal{P}(\hat{\varepsilon}^*(P, -1)) + O(k^2), \\ \sqrt{\frac{2M}{2m_b 2m_c}} \frac{1}{\sqrt{2}} \{v'_b(p_b + k, +)\bar{u}'_c(p_c - k, +) + v'_b(p_b + k, -)\bar{u}'_c(p_c - k, -)\} &= \\ &= \mathcal{P}(\hat{\varepsilon}^*(P, 0)) + O(k^2), \\ \sqrt{\frac{2M}{2m_b 2m_c}} v'_b(p_b + k, -)\bar{u}'_c(p_c - k, +) &= \\ &= \mathcal{P}(\hat{\varepsilon}^*(P, +1)) + O(k^2). \end{aligned} \quad (5)$$

In the B_c rest frame, the polarization vectors of the spin-triplet state have the form

$$\begin{aligned} \varepsilon^{rf}(-1) &= \frac{1}{\sqrt{2}}(0, 1, -i, 0), \\ \varepsilon^{rf}(0) &= (0, 0, 0, 1), \\ \varepsilon^{rf}(+1) &= -\frac{1}{\sqrt{2}}(0, 1, i, 0). \end{aligned} \quad (6)$$

In calculations the Dirac representation of γ -matrices is used and the following explicit form of the spinors is applied

$$\begin{aligned} u(p, +) &= \frac{1}{\sqrt{E+m}} \begin{pmatrix} E+m \\ 0 \\ p_z \\ p_x + ip_y \end{pmatrix}, & u(p, -) &= \frac{1}{\sqrt{E+m}} \begin{pmatrix} 0 \\ E+m \\ p_x - ip_y \\ -p_z \end{pmatrix} \\ v(p, +) &= -\frac{1}{\sqrt{E+m}} \begin{pmatrix} p_z \\ p_x + ip_y \\ 0 \\ E+m \end{pmatrix}, & v(p, -) &= \frac{1}{\sqrt{E+m}} \begin{pmatrix} p_x - ip_y \\ p_z \\ 0 \\ E+m \end{pmatrix} \end{aligned} \quad (7)$$

For the P -wave states in eq.(1), the $T^{Ss_z}(p_i, k(\mathbf{q}))$ amplitude can be expanded into the Taylor series up to the terms linear over \mathbf{q} . Then one gets

$$A^{SJj_z} = iR'_P(0) \sqrt{\frac{2M}{2m_b 2m_c}} \sqrt{\frac{3}{4\pi}} C_{s_z l_z}^{Jj_z} \mathcal{L}^{l_z}(T^{Ss_z}(p_i, k(\mathbf{q}))), \quad (8)$$

where $R'_P(0)$ is the first derivative of the radial wave function at the origin, and \mathcal{L}^{l_z} has the following form

$$\begin{aligned}\mathcal{L}^{-1} &= \frac{1}{\sqrt{2}} \left(\frac{\partial}{\partial q_x} + i \frac{\partial}{\partial q_y} \right), \\ \mathcal{L}^0 &= \frac{\partial}{\partial q_z}, \\ \mathcal{L}^{+1} &= -\frac{1}{\sqrt{2}} \left(\frac{\partial}{\partial q_x} - i \frac{\partial}{\partial q_y} \right),\end{aligned}\tag{9}$$

where $\frac{\partial}{\partial q_x}$, $\frac{\partial}{\partial q_y}$, $\frac{\partial}{\partial q_z}$ are the differential operators acting on $T^{Ss_z}(p_i, k(\mathbf{q}))$ as the function of $\mathbf{q} = (q_x, q_y, q_z)$ at $\mathbf{q} = 0$.

As all considered matrix elements are calculated in the system distinct from the B_c rest frame, the four-momentum $k(\mathbf{q})$ has been calculated by the following formulae

$$\begin{aligned}k^0 &= \frac{\mathbf{v} \cdot \mathbf{q}}{\sqrt{1-\mathbf{v}^2}}, \\ \mathbf{k} &= \mathbf{q} + \left(\frac{1}{\sqrt{1-\mathbf{v}^2}} - 1 \right) \frac{\mathbf{v} \cdot \mathbf{q}}{\mathbf{v}^2} \mathbf{v},\end{aligned}\tag{10}$$

where \mathbf{v} is the B_c velocity in the system, where the calculations are performed. The matrix element $T^{Ss_z}(p_i, k(\mathbf{q}))$ is computed, so that the four-momenta of \bar{b} and c quarks are determined by eq.(2), taking into account eq.(10).

The first derivatives in eq.(9) are substituted by the following approximations

$$\frac{\partial T^{Ss_z}(p_i, k(\mathbf{q}))}{\partial q_j} \Big|_{\mathbf{q}=\mathbf{0}} \approx \frac{T^{Ss_z}(p_i, k(\mathbf{q}^j)) - T^{Ss_z}(p_i, 0)}{\Delta},\tag{11}$$

where Δ is some small value, and \mathbf{q}^j have the following form

$$\begin{aligned}\mathbf{q}^x &= (\Delta, 0, 0), \\ \mathbf{q}^y &= (0, \Delta, 0), \\ \mathbf{q}^z &= (0, 0, \Delta).\end{aligned}\tag{12}$$

With the chosen values of quark masses and interaction energies, the increment value $\Delta = 10^{-5}$ GeV has provided the stability of 4-5 meaning digits in the squared matrix elements summed over j_z for all P -wave states with the given value of J and S , when one has performed the Lorentz transformations along the beam axis or the rotation around the same axis.

One has to note that because of such transformations, the new vectors $k(\mathbf{q}^j)$ do not correspond to the transformed old vectors. Therefore, the applied test is not only a check of the correct typing of the $T^{Ss_z}(p_i, k(\mathbf{q}))$ amplitude, but it is also the check of correct choice of the phases in eq.(8).

The matrix element A^{SJj_z} squared, which is calculated by the method described above, must be summed over j_z as well as the spin states of free b and \bar{c} quarks. It also must be averaged over spin projections of initial particles.

The phase space integration has been made by the Monte Carlo method of RAMBO program [8].

III. DISCUSSION OF RESULTS

To check the numerical way of the amplitude calculation for the P -wave level production of B_c , we have considered the production of these states in e^+e^- annihilation, where the analytical expressions for the differential cross-sections were derived in the $M^2/s \ll 1$ limit [5]. Those expressions define the functions of the $\bar{b} \rightarrow B_c(L=1)$ fragmentation. It should be noted that in the accurate consideration of the fragmentation mechanism for the $B_c(L=1)$ production in $e^+e^- \rightarrow \gamma^* \rightarrow B_c + X$, one can see that in addition to the \bar{b} fragmentation one has to account for the c quark fragmentation into B_c . Moreover, the most significant role is played by the c fragmentation into 3P_0 state. Therefore, to compare with the numerical results we use the analytical expressions accounting for both \bar{b} and c fragmentation. As one can see in Fig.1, the distributions of 1P_1 , 3P_0 , 3P_1 , 3P_2 level 1 production, $d\sigma/dz$ ($z = 2|\mathbf{P}_{B_c}|/\sqrt{s}$ with

¹In the $\bar{b}c$ system the quark spin-dependent corrections to the heavy quarkonium potential lead to the mixing of 3P_1 and 1P_1 levels [9]. In the fragmentation model this mixing results in redefinition of corresponding frag-

\mathbf{P}_{B_c} being the three-momentum of B_c meson in the c.m.s.), calculated numerically and given analytically, coincide with each other at the same set of parameters, which are give below

$$\begin{aligned}
\alpha_{em} &= 1/128, \\
\alpha_s &= 0.2, \\
m_b &= 5.0 \text{ GeV}, \\
m_c &= 1.7 \text{ GeV}, \\
|R'_P(0)|^2 &= 0.201 \text{ GeV}^5.
\end{aligned}
\tag{13}$$

Thus, the performed verification convinces us that the calculation method used is quite accurate.

Let us consider the P -wave level production of B_c in $\gamma\gamma$ collisions. The cross-section of the P -wave level production at various energies of interacting photons are presented in Tab.1 and Fig.2. One can see in Fig.2 that in the region of interest the energy dependence of the summed cross-section at the chosen m_b and m_c values is quite accurately described by the following approximation, shown as solid line in Fig.2,

$$\sigma_{B_c(L=1)} = 130 \cdot \left(1 - \left(\frac{2(m_b + m_c)}{\sqrt{s}} \right)^2 \right)^{2.7} \cdot \left(\frac{2(m_b + m_c)}{\sqrt{s}} \right)^{1.32} \text{ fb}.
\tag{14}$$

The summed fragmentation contribution, obtained as the product of the $\gamma\gamma \rightarrow b\bar{b}$ and $\gamma\gamma \rightarrow c\bar{c}$ cross-sections and the corresponding probabilities of the fragmentation ($5.34 \cdot 10^{-5}$ for the \bar{b} quark fragmentation and $1.58 \cdot 10^{-6}$ for the c quark one, respectively), is shown in the same figure. One can see in Fig.2 that the fragmentation contribution, evaluated in the model, is small at high energies, where the application of this model could be sound for the \bar{b} fragmentation, at least. The fragmentation model overestimates the exact result obtained over the complete set of leading order diagrams at low energies close to $\sqrt{s} \leq 30$ GeV. This overestimation has a simple explanation and it is related with incorrect evaluation of phase space, since in the fragmentation model, one uses the two-particle phase space instead of the three-particle one in the exact calculations. For the correct study of the fragmentation mechanism the $M^2/s \ll 1$ condition is necessary to be satisfied. Therefore, in what follows, we will restrict ourselves by the consideration of differential distributions at $\sqrt{s} = 100$ GeV, where the mentioned condition is certainly valid.

The $d\sigma/dz$ distribution for 1P_1 state production cross-section in $\gamma\gamma$ collisions is shown as the solid line histogram in Fig.3a. The dashed line histogram in the same figure denotes the gauge invariant contribution of six diagrams, where the $c\bar{c}$ pair is emitted from the b or \bar{b} quark line, i.e. the \bar{b} quark fragmentation into B_c meson takes place. This exactly calculated term is compared with the prediction of fragmentation model, considered in [5] and presented as the smooth dashed curve. One can see that the exact result for $\bar{b} \rightarrow B_c$ is quite accurately described by analytical expression of fragmentation model, whereas the c fragmentation diagrams contribution, shown as the dotted line histogram, is larger than the predictions of fragmentation model, so that in absolute values, it is larger than the \bar{b} quark fragmentation term. Remember, that the analogous picture takes place also for the photonic production of S -wave states of B_c meson [6]. One can see in Fig.3a, that as well as in the production of S -wave levels, the fragmentation contribution does not dominate, and the main contribution is determined by the recombination diagrams. However, for the correct study of the fragmentation mechanism in photon-photon collisions, one must consider the spectra not over the total energy of the meson, but over its transverse momentum, giving an additional scale of energy, so that one can expect the factorization of the heavy quark hard production at large $P_T \gg M_{B_c}$ and the forthcoming fragmentation, where the particle virtualities are of the order of the quark masses.

The cross-section distributions over the transverse momentum of 1P_1 level of the B_c meson are shown in Fig.3b. The solid line histogram denotes the result of calculations over the complete set of diagrams, the dashed histogram and curve show the contribution by the \bar{b} fragmentation diagrams and the prediction of fragmentation model, correspondingly, and the c fragmentation diagram contribution (the dotted

mentation functions, i.e. in the introduction of additional functions for the 1^+ and $1^{+'}$ states [5]. However, first, the mixing effect does not influence the consideration of the physical mechanism of photonic production of the P -wave states, and second, in the studied approach the $^S P_J$ -state masses are degenerated over J , so that the isolation of the $S = 0$ and $S = 1$ components in the $J = 1$ state is rather conventional. That is why we restrict ourselves by the consideration of distributions for the $^S P_J$ states.

histogram) is compared with the corresponding prediction of fragmentation model (the dotted curve) at $\sqrt{s} = 100$ GeV.

As well as in the S -wave state production, the fragmentation mechanism does not dominate even at large P_T .

The analogous distributions for the 3P_0 , 3P_1 , 3P_2 states are presented in Figs.4a-6b. In Figs.5-6, where the 3P_1 , 3P_2 spectra are shown, one can draw the conclusions, which repeat the statements concerning the 1P_1 production. The picture of the 3P_0 meson production slightly differs from the general case. As one can see in Fig.4b, the \bar{b} quark fragmentation at large transverse momenta plays a much greater role than that in the production of other P -wave levels, while, contrary, the diagrams corresponding to the c fragmentation, are less essential than in other cases.

IV. CONCLUSION

In this paper we have performed the numerical calculation for the P -wave level production of B_c mesons in $\gamma\gamma$ collisions in the leading $O(\alpha_s^2\alpha_{em}^2)$ order of the perturbation theory. From the theoretical point of view, the consideration of $\gamma\gamma$ collisions in this respect is of special interest, since, on the one hand, in the photonic production of B_c as well as in e^+e^- annihilation, one can isolate the gauge invariant set of fragmentational diagrams, and, on the other hand, there is also the contribution of recombination type diagrams, which are essential in the consideration of a more complicated case of the hadronic B_c production [7].

The performed calculations show that:

1. The total cross-section of P -wave state production of B_c is about 10 % in respect to the production of S -wave levels, as it takes place in e^+e^- annihilation.
2. As well as in the S -wave level production, the recombination mechanism dominates, and the fragmentation one is small.
3. The \bar{b} fragmentation diagram contribution is quite accurately described by the fragmentation function at large P_T as well as low one, whereas for the c fragmentation diagrams, the fragmentational picture is broken completely.

This work is supported, in part, by the International Science Foundation grants NJQ000 and NJQ300. The work of A.V. Berezhnoy has been made possible by a fellowship of INTAS Grant 93-2492 and one of International Soros Science Education Program Grant A1377 and is carried out within the research program of International Center for Fundamental Physics in Moscow.

REFERENCES

1. Gershtein S.S., Kiselev V.V., Likhoded A.K., Tkabladze A.V.// Uspekhi Fiz. Nauk. 1995. V. 165. P. 3.
2. Clavelli L.// Phys. Rev. 1982. V. D26. P. 1610; Ji C.-R. and Amiri R.// Phys. Rev. 1987. V. D35. P. 3318; Chang C.-H. and Chen Y.-Q.//Phys. Lett. 1992. V. B284 P. 127.
3. Braaten E., Cheung K., Yuan T.C.// Phys.Rev. 1993. V. D48. P. 4230.
4. Kiselev V.V., Likhoded A.K., Shevlyagin M.V.// Z.Phys. 1994. V. C63. P. 77.
5. Yuan T.C.// Phys.Rev. 1994. V. D50. P. 5664.
6. Berezhnoy A.V., Likhoded A.K., Shevlyagin M.V.// Phys.Lett. 1995. V. B342. P. 351; Kolodziej K., Leike A., Rückl R.// Preprint MPI-PhT/94-84, LMU-23-94, 1994.
7. Berezhnoy A.V., Likhoded A.K., Shevlyagin M.V.// Yad.Fiz. 1995. V. 58. P. 730; Berezhnoy A.V., Likhoded A.K., Yushchenko O.P.// Preprint IHEP 95-59. Protvino, 1995; hep-ph/9504302; Kolodziej K., Leike A., Rückl R.// Preprint MPI-PhT/95-36, 1995; hep-ph/9505298.
8. Kleiss R., Stirling W.J., Ellis S.D.// Comp. Phys. Commun. 1986. V. 40. P. 356.

TABLE I. The dependence of production cross-sections for different P -wave states of B_c on the total energy of colliding photons. (The calculation errors are shown in parenthesis).

\sqrt{s} , GeV	σ_{1P_1} , fb	σ_{3P_0} , fb	σ_{3P_1} , fb	σ_{3P_2} , fb
15.	1.064(2)	0.1329(3)	0.08707(18)	0.894(2)
20.	5.703(11)	0.968(2)	1.147(2)	8.098(15)
30.	7.56(3)	1.409(5)	2.84(1)	12.11(5)
40.	6.72(4)	1.269(9)	3.063(18)	11.01(7)
60.	4.68(5)	0.882(12)	2.42(3)	7.7(1)
80.	3.32(5)	0.624(15)	1.80(3)	5.48(12)
100.	2.58(3)	0.493(9)	1.42(2)	4.32(7)

FIGURE CAPTIONS

Fig. 1. The B_c production cross-section distributions over z in the $e^+e^- \rightarrow \gamma^* \rightarrow B_c + X$ process are presented as the histograms in comparison with the fragmentation model predictions shown as the smooth curves, at $\sqrt{s} = 100$ GeV for the following B_c states: 1P_1 (solid line), 3P_0 (dashed line), 3P_1 (dotted line), 3P_2 (dotted-dashed line).

Fig. 2. The summed cross-section dependence of P -wave states on the energy of interacting photons is marked by (\bullet) in comparison with the prediction of \bar{b} and c quark fragmentation model (dashed curve). The solid line corresponds to the approximation of (14).

Fig. 3. a. The z distributions, corresponding to the photonic production of 1P_1 state at the interaction energy 100 GeV. The total result is presented by the solid line histogram, the b fragmentation diagrams contribution (dashed histogram) is compared with the prediction of fragmentation model (dashed curve), the c fragmentation diagrams term is denoted as the dotted histogram in comparison with the fragmentation model result (dotted curve).

b. The transverse momentum distributions, corresponding to the photonic production of 1P_1 state at the interaction energy 100 GeV. The notations of different contributions are the same as in Fig. 3a.

Fig. 4a,b. The 3P_0 spectra, denoted as in Fig.3a,b.

Fig. 5a,b. The 3P_1 spectra, denoted as in Fig.3a,b.

Fig. 6a,b. The 3P_2 spectra, denoted as in Fig.3a,b.

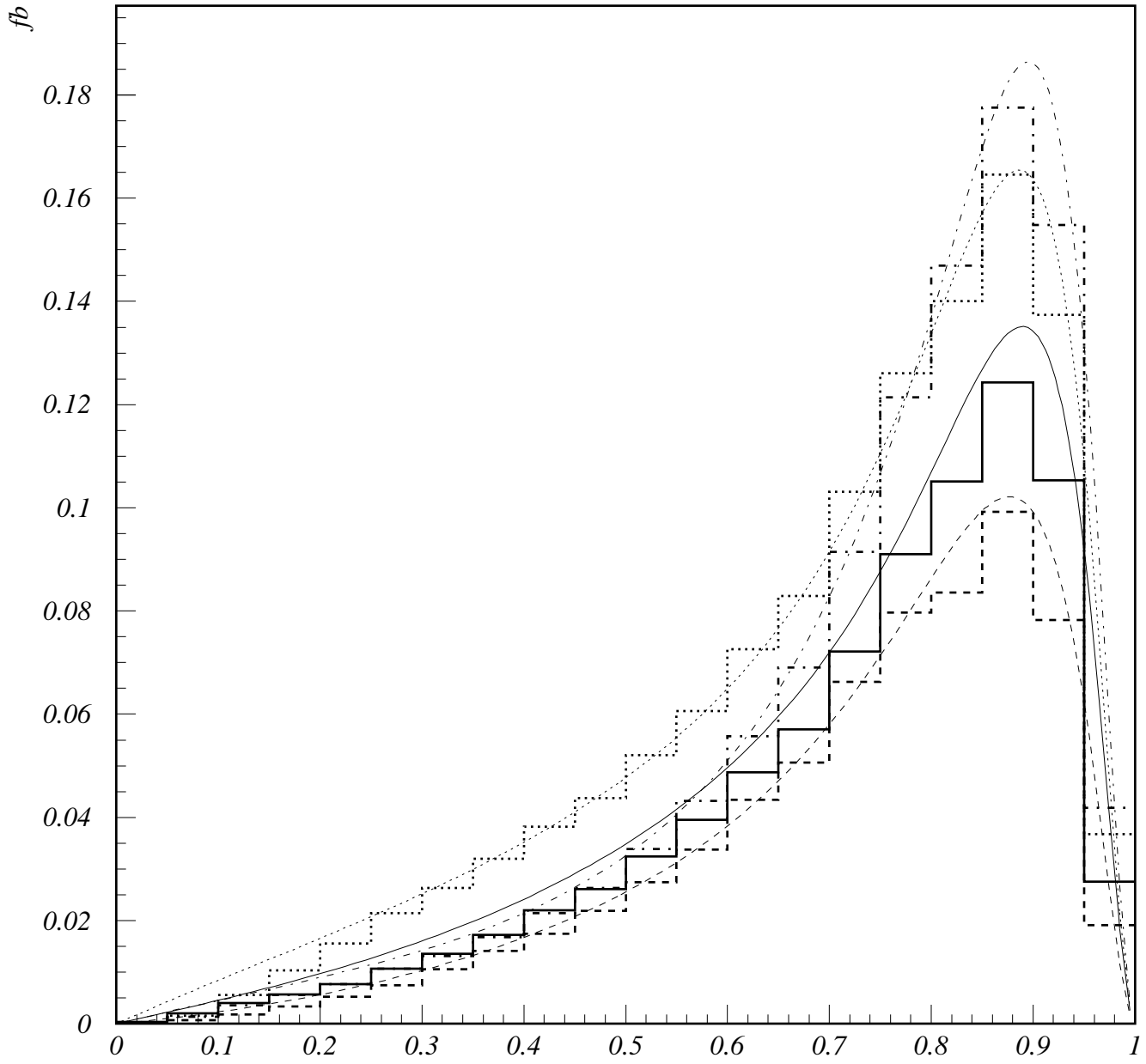


Fig.1

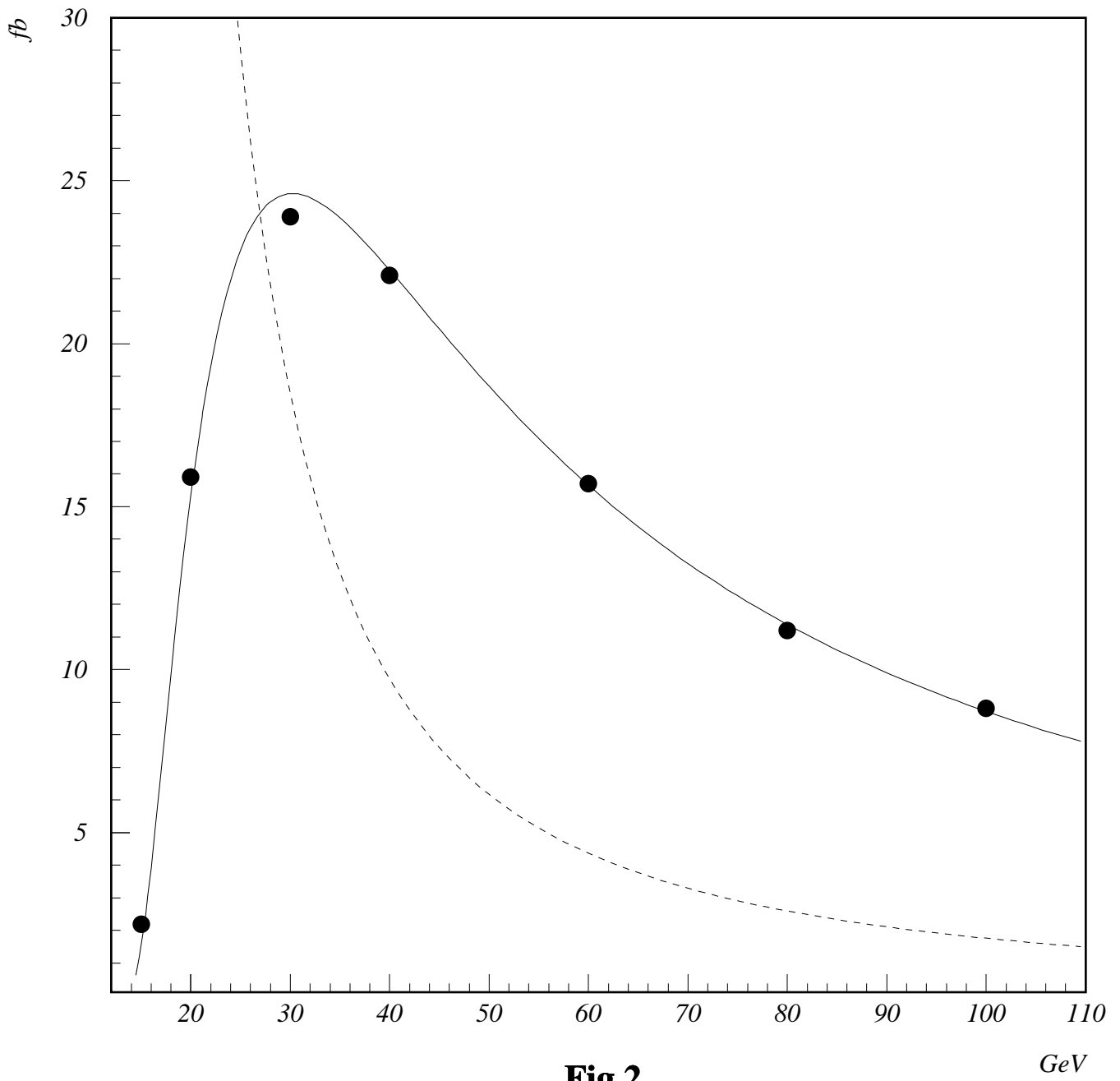


Fig.2

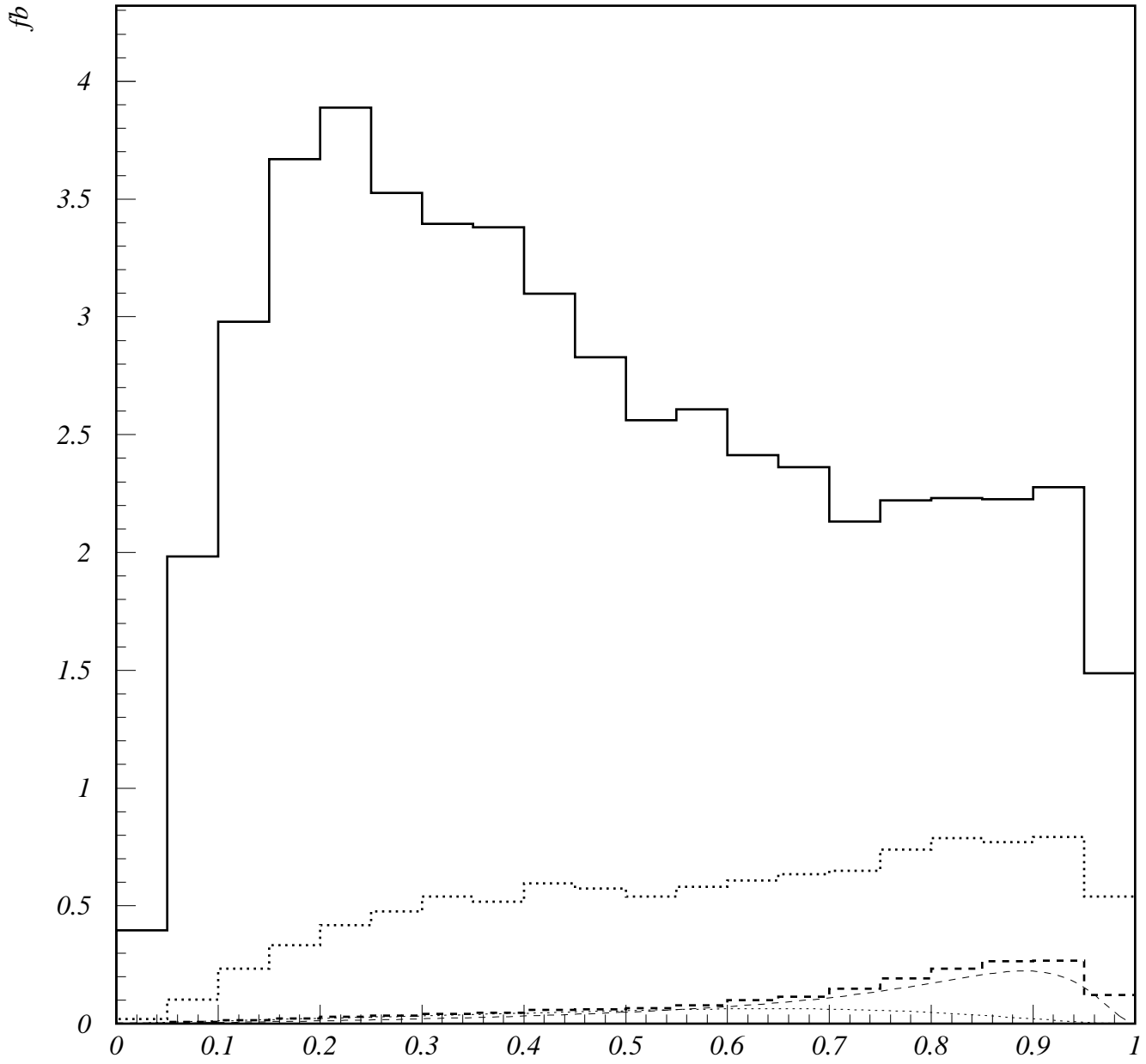


Fig.3a

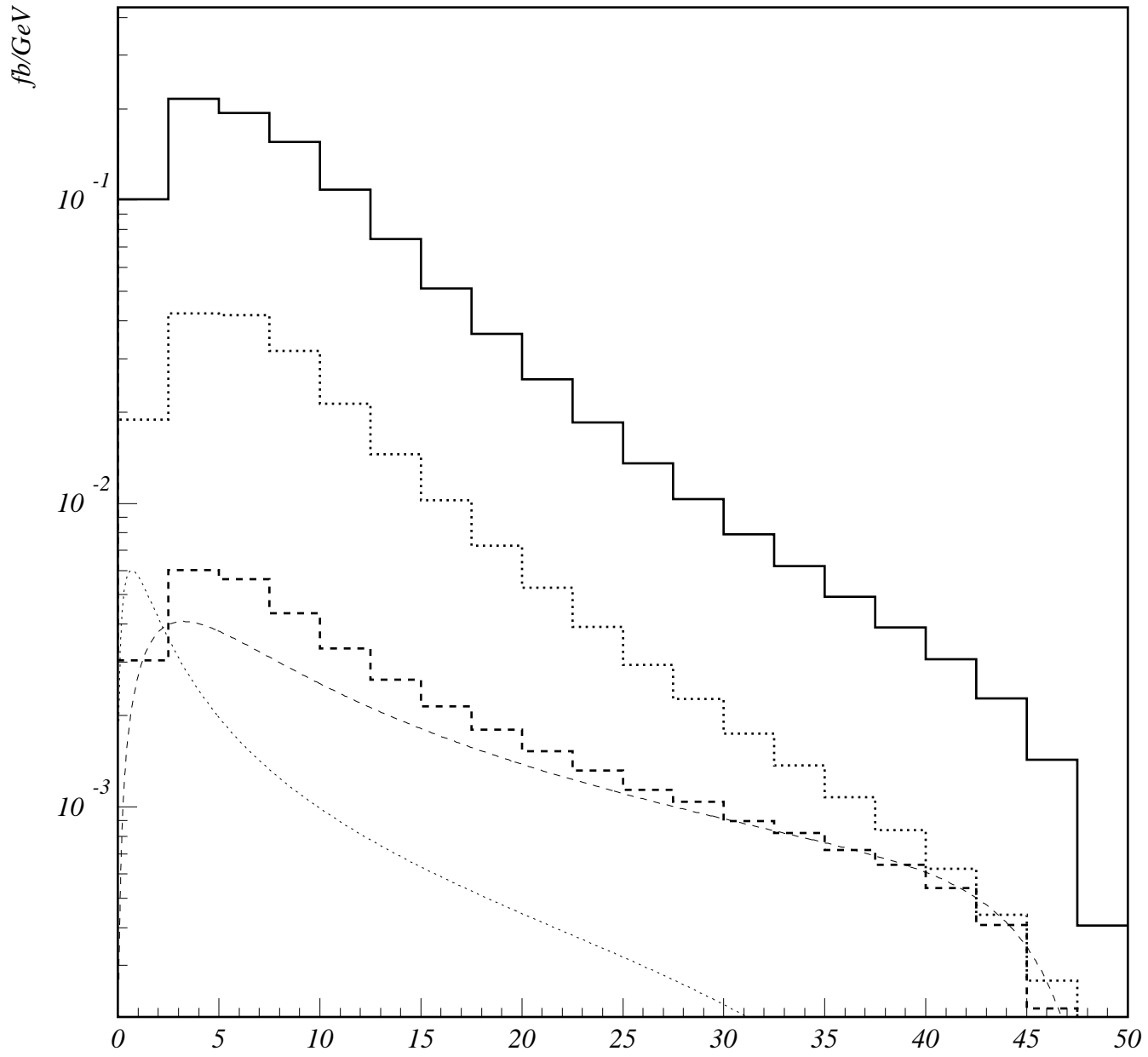


Fig.3b

GeV

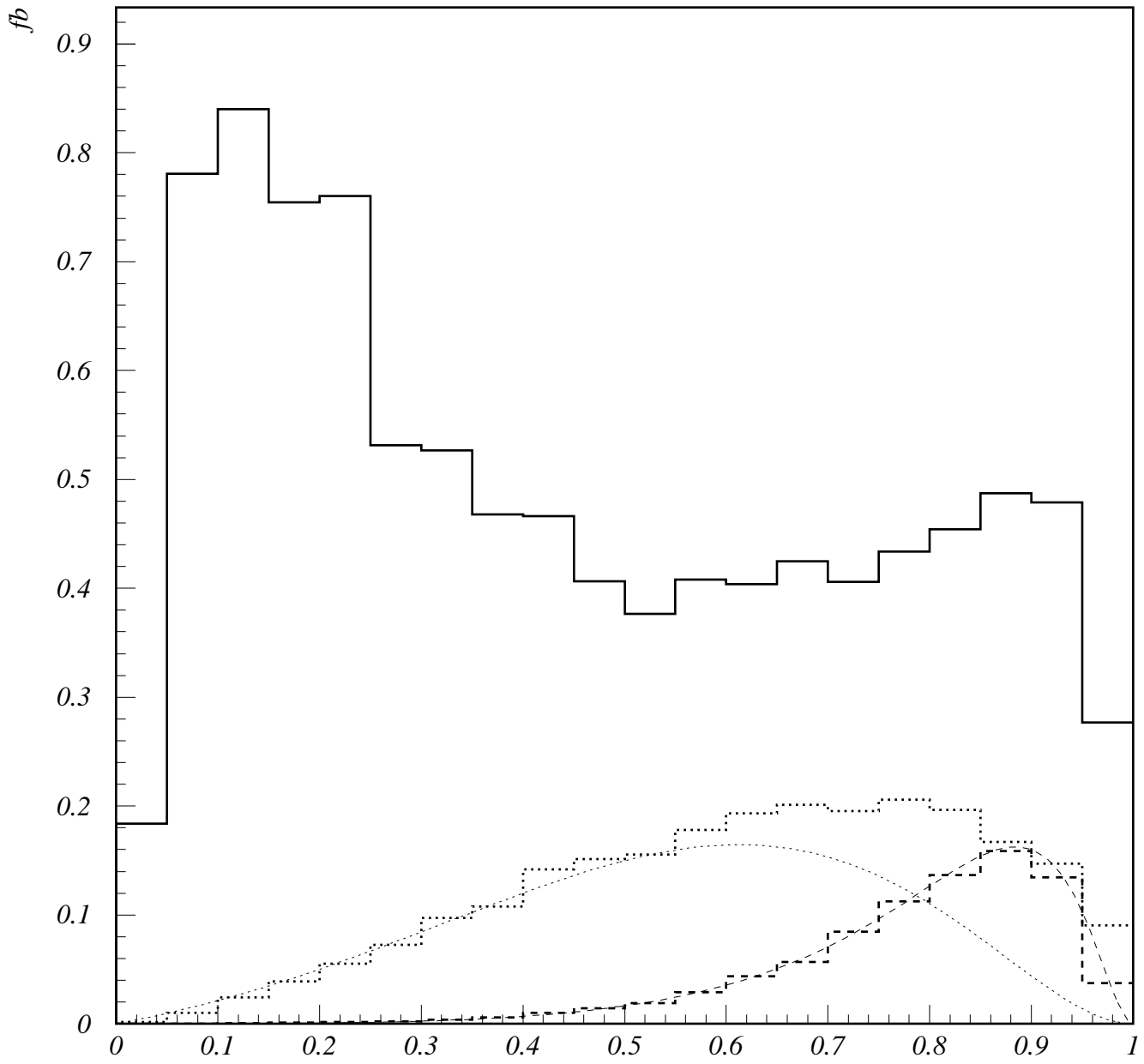


Fig.4a

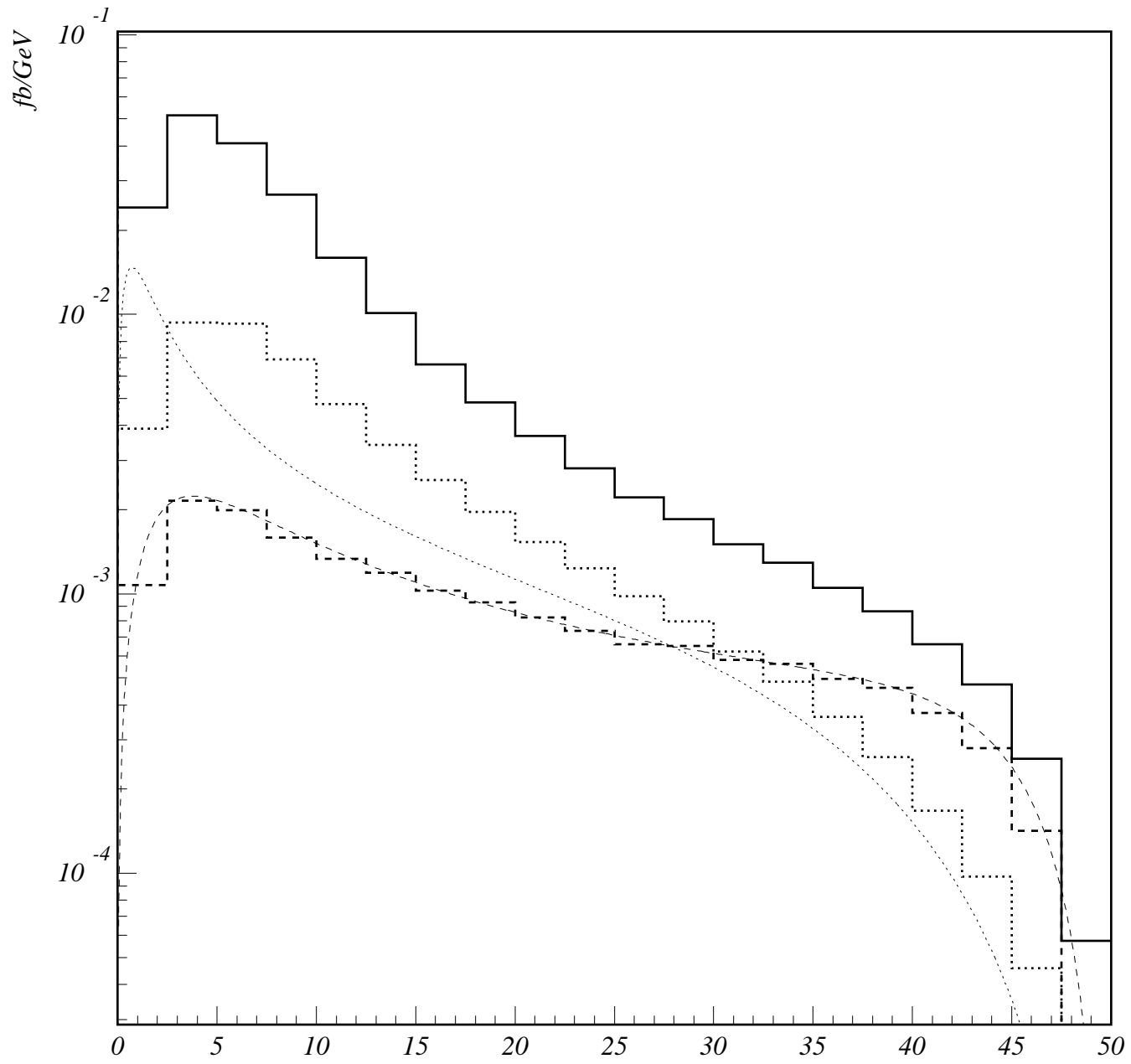


Fig.4b

GeV

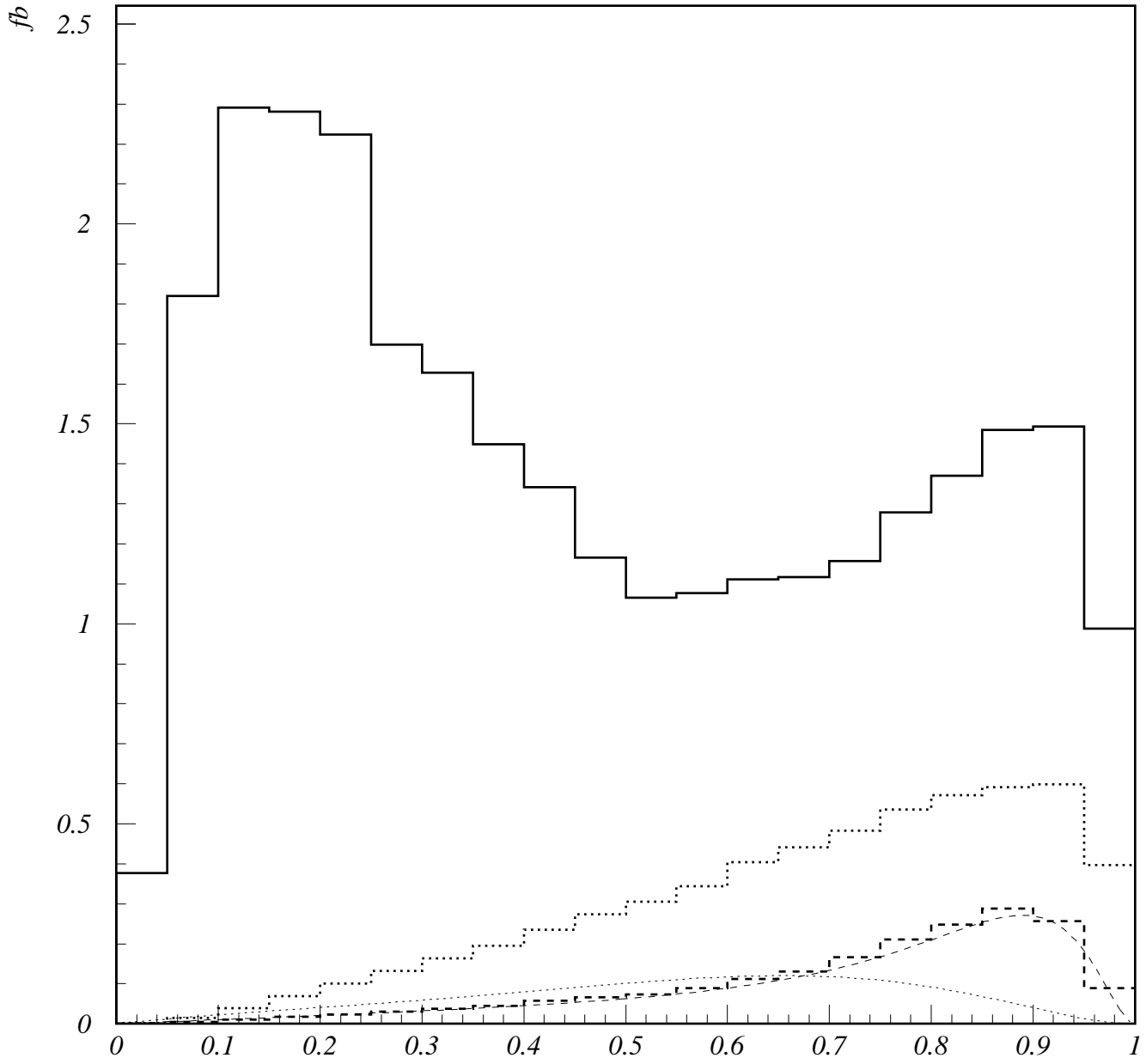


Fig.5a

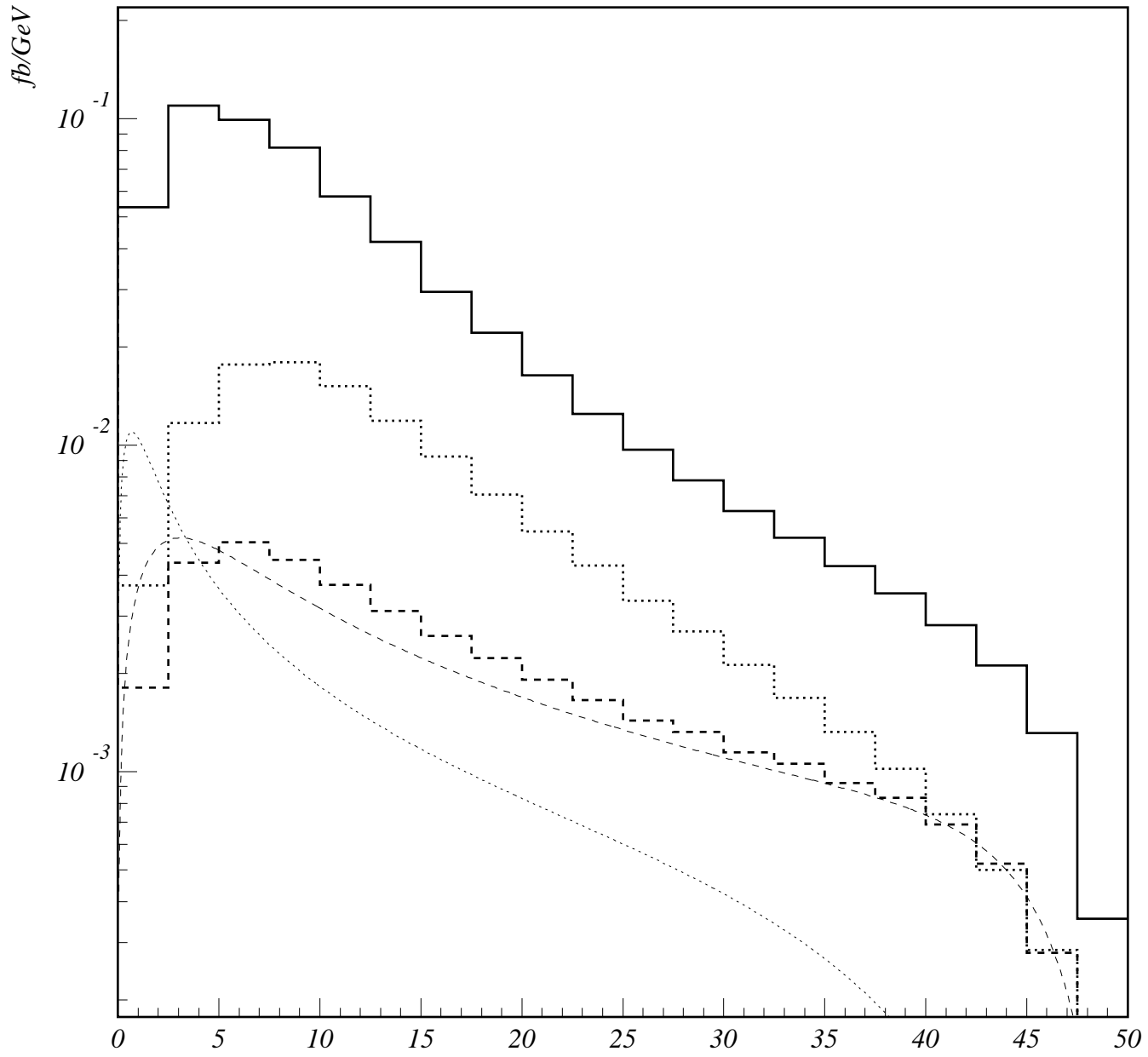


Fig.5b

GeV

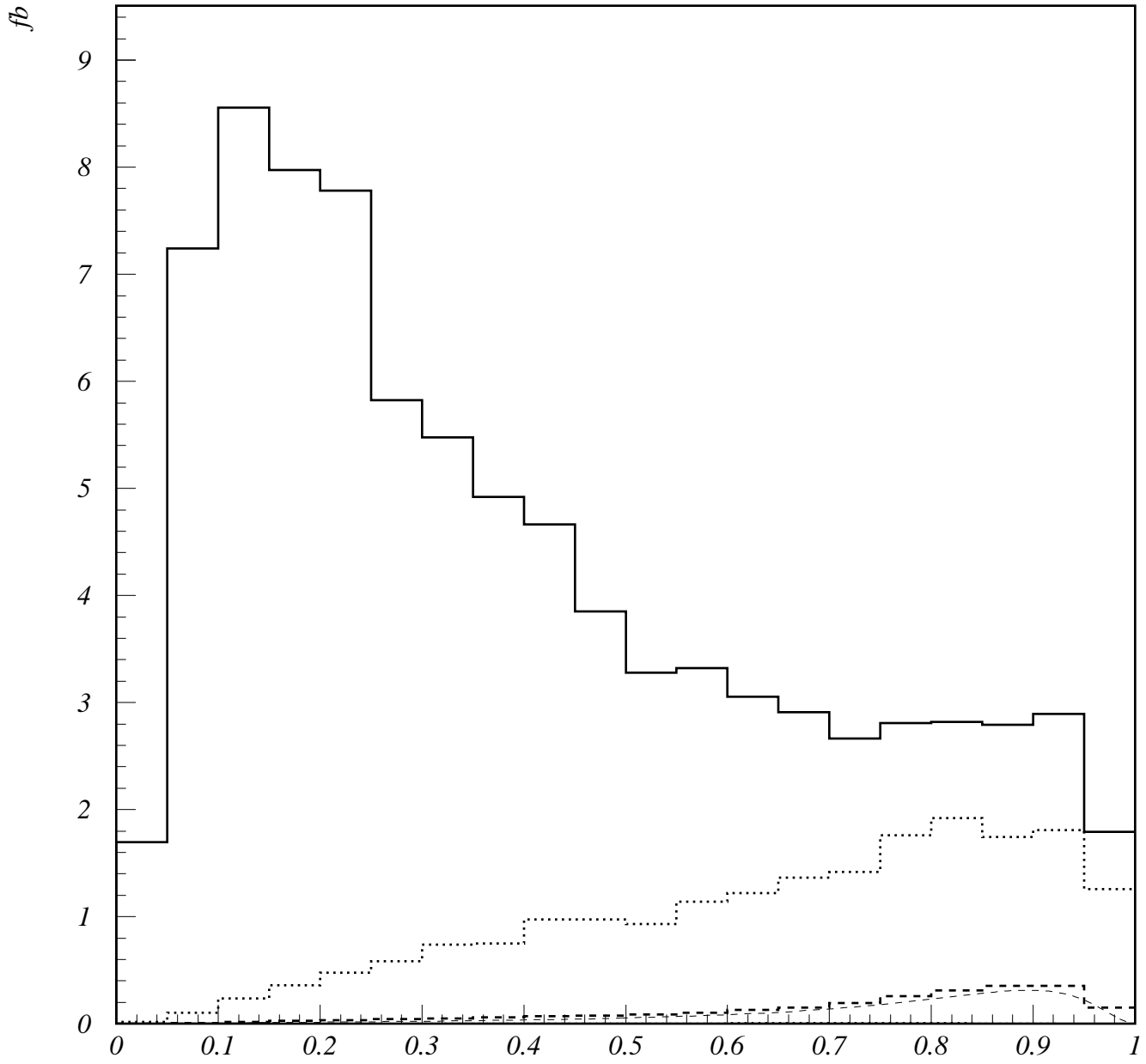


Fig.6a

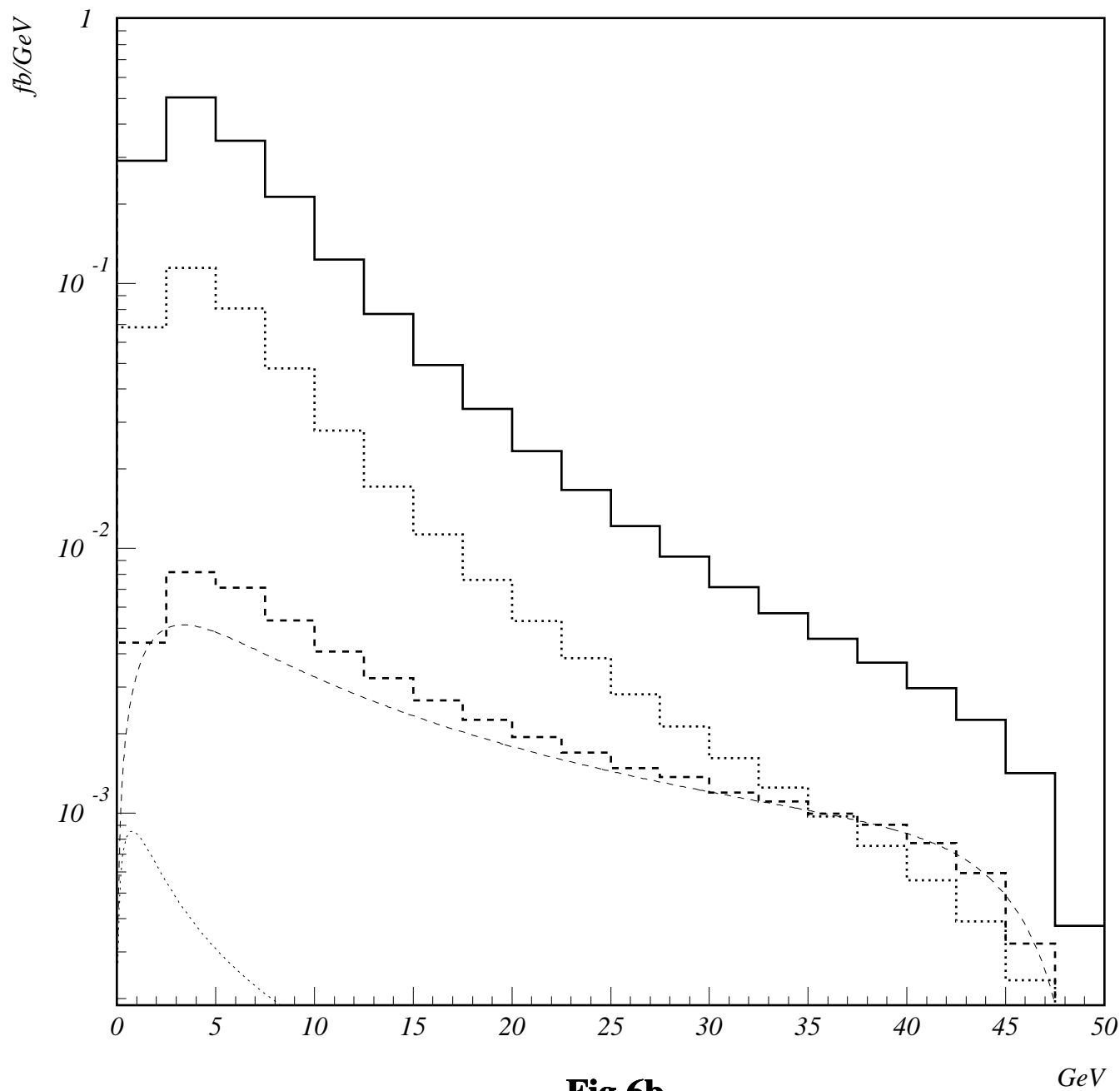


Fig.6b

GeV